ANNALS OF GEOPHYSICS, 68, 2, S217, 2025; doi:10.4401/ag-9246
OPEN ACCESS

Integrated Earthquake Risk Assessment Using PSHA-Based Microzonation and Soil Vulnerability Index Maps of Urban Kathmandu Valley

Dibyashree Poudyal[*,1], Norhaiza Nordin[1], Siti Nur Aliaa Roslan[2]

(1) Infrastructure University Kuala Lumpur, Department of Civil Engineering, Kajang, Malaysia
(2) Universiti Putra Malaysia, Department of Civil Engineering, Serdang, Malaysia

Article history: received January 15, 2025; accepted March 18, 2025

Abstract

The Kathmandu Valley, located in a seismically active region, has a long history of enduring significant earthquakes. Despite existing efforts, previous studies often lack comprehensive integration of seismic hazard data with vulnerability assessment, which is crucial for detailed earthquake risk evaluations. This study develops a comprehensive seismic risk assessment by integrating probabilistic seismic hazard analysis (PSHA) and soil vulnerability index map using Arc GIS. The PSHA, conducted with the R-CRISIS tool, estimates peak ground acceleration (PGA) across the region, while the soil vulnerability index is derived from nonlinear ground response analysis using DEEPSOIL. The seismic hazard analysis, reveals maximum peak ground accelerations (PGA) ranging from 0.345 g to 0.382 g over 50 years at a 10% probability of exceedance, corresponding to a return period of 475 years. The soil vulnerability index extending from 0.21 to 21.72, is applied here to assess the risk. Among the metropolitan cities and municipalities, Madhyapur Thimi emerged as the safest area, with 99.38% of its region classified as low-risk, while Shankharapur municipality was identified as the most vulnerable, with 88.01% of its area classified as high-risk. This study provides critical insights for seismic risk assessment in the Kathmandu Valley; however, further research should consider dynamic land use and urban development changes to continually refine and update these assessments.

Keywords: Amplification factor; dominant frequency; PGA; PSHA; Vulnerability index

1. Introduction

The analysis of seismic hazards is a useful tool for illustrating the potentially harmful effects of earthquakes. In addition to causing buildings to collapse as a result of ground shaking, earthquake disasters can also cause liquefaction, landslides, and fire. Therefore, it is essential to predict the ground shaking level in advance to meet technical requirements for reducing the risk of earthquakes. The Kathmandu Valley has experienced a number of strong earthquakes over the years. The most notable earthquake is the 2015 Gorkha earthquake. The likelihood of an earthquake calamity in the Kathmandu Valley is influenced by the convergence of the Indian and Tibetan plates and thick soft soil sediments make the scenario more dangerous for cities close to the Himalayan region

(Anbazhagan et al., 2019). A major earthquake is likely to occur soon since the 2015 Gorkha earthquake in Nepal was unable to completely breach the primary fault beneath the Himalayan region (Anbazhagan et al., 2017). The heightened population density compared to previous significant earthquakes has increased the vulnerability of the region to seismic hazards. The impacts of a seismic event extend beyond structural collapse and can include phenomena such as soil liquefaction, sand boiling, and landslides.

BECA (1993) conducted an early probabilistic seismic hazard analysis (PSHA) and risk assessment for Nepal, which contributed to the development of the Nepal Building Code (NBC 105, 1994). However, subsequent studies by various researchers (Parajuli et al., 2021; Rahman et al., 2018; Stevens et al., 2018; Thapa and Guoxin, 2013) have also performed PSHA for Nepal. These studies used different earthquake sources and ground motion predictive equations (GMPEs), resulting in varying peak ground accelerations (PGA) at the same regions. The seismic hazard studies conducted in Nepal by Pradhan et al. (2020), Bhusal and Parajuli (2019), Moklesur et al. (2018) and Thapa (2013) and Guoxin (2013) share a common objective of assessing seismic risks across the region, yet they differ significantly in their methodologies, data processing, and geographic focus. Moklesur et al. (2018) utilized a more nuanced approach by integrating three distinct seismogenic source models reflecting the complex tectonics of the region. This study highlighted the high seismic hazard potential in the Lesser Himalayas, with significant spatial variations, particularly along the Main Himalayan Thrust. While, Bhusal et al., (2022) conducted a PSHA for the Dharahara monument in Kathmandu, Nepal to develop an elastic response spectrum for the bedrock site. The resulting spectrum was then compared with the current seismic codes, NBC 105 (2020) and IS 1893:2016, to establish the target response spectrum.

A series of studies conducted in the aftermath of the 2015 Gorkha earthquake in Nepal addressed various aspects of seismic activity and its impacts. Most of the existing seismic assessments in Nepal focused on various forms of vulnerability including social vulnerability, climate change, flood risk, landslides, liquefaction, fire, and extreme weather events for different districts of Nepal. In addition, Khatakho et al. (2021) performed a multi-hazard risk assessment in Kathmandu Valley, using the Analytical Hierarchy Process (AHP) and GIS, integrating flood, landslide, earthquake, and urban fire hazards to identify areas with high to very high levels of risk, particularly in densely populated and central valley regions. Bhochhibhoya and Maharjan (2022) conducted a district-level seismic risk assessment in Nepal by integrating physical earthquake hazards with social vulnerability factors to develop a combined vulnerability score using Open Quake and ArcGIS. These studies show that earthquake risk assessments in Nepal have been conducted to a limited extent.

In contrast to the study by (Khatakho et al., 2021) which categorized the valley area into different degrees of hazard levels, this study further refines the analysis by integrating the hazard and soil vulnerability index and classifying risk zones as low, medium, and high within the municipalities and metropolitan cities of the Valley. This granular approach allows for a more nuanced understanding of the varying degrees of risk across different administrative units within the Kathmandu Valley. Additionally, there are several studies related to different earthquakes for instance Kobe earthquake, Uttarkashi earthquake, and Chamauli earthquake, etc, none of them can be compared with the Peak ground acceleration (PGA) of the Gorkha earthquake because of variations in parameters such as magnitude, focal depth, epicentral distance, faulting mechanism, geological conditions and building construction techniques. Various factors make each earthquake event different in as much as the ground shaking intensity and the extent to which PGA experienced are concerned. Despite Nepal having experienced several major earthquakes, including the 1934 earthquake, due to the lack of well-documented records, input motion Gorkha earthquake has been selected for this study to acquire a closer depiction of seismic hazards relevant to the study area. Therefore, by combining the hazard and soil vulnerability index map at the municipal level and metropolitan centers of the Kathmandu Valley, this study fills a major gap in seismic risk assessment. For increased accuracy, the Gorkha earthquake is used as the input motion. Furthermore, by addressing the shortcomings noted in earlier research, this study offers insightful information that can guide more focused approaches to disaster planning and mitigation that are adapted to the unique hazards that each municipality and metropolitan area faces.

1.1 Seismicity of the study area

Seismic features, including faults, shear zones, and lineaments, must be included in all earthquake events that have occurred in the study region to conduct seismic hazard analysis (Anbazhagan et al., 2015). The Kathmandu Valley comprises the metropolitan cities of Kathmandu, Lalitpur, and Bhaktapur district, along with the municipalities of Madhyapur Thimi, Kirtipur, Shankharapur, Gokarneshwor, Kageshwori Manohara, Tarkeshwor, Chandragiri,

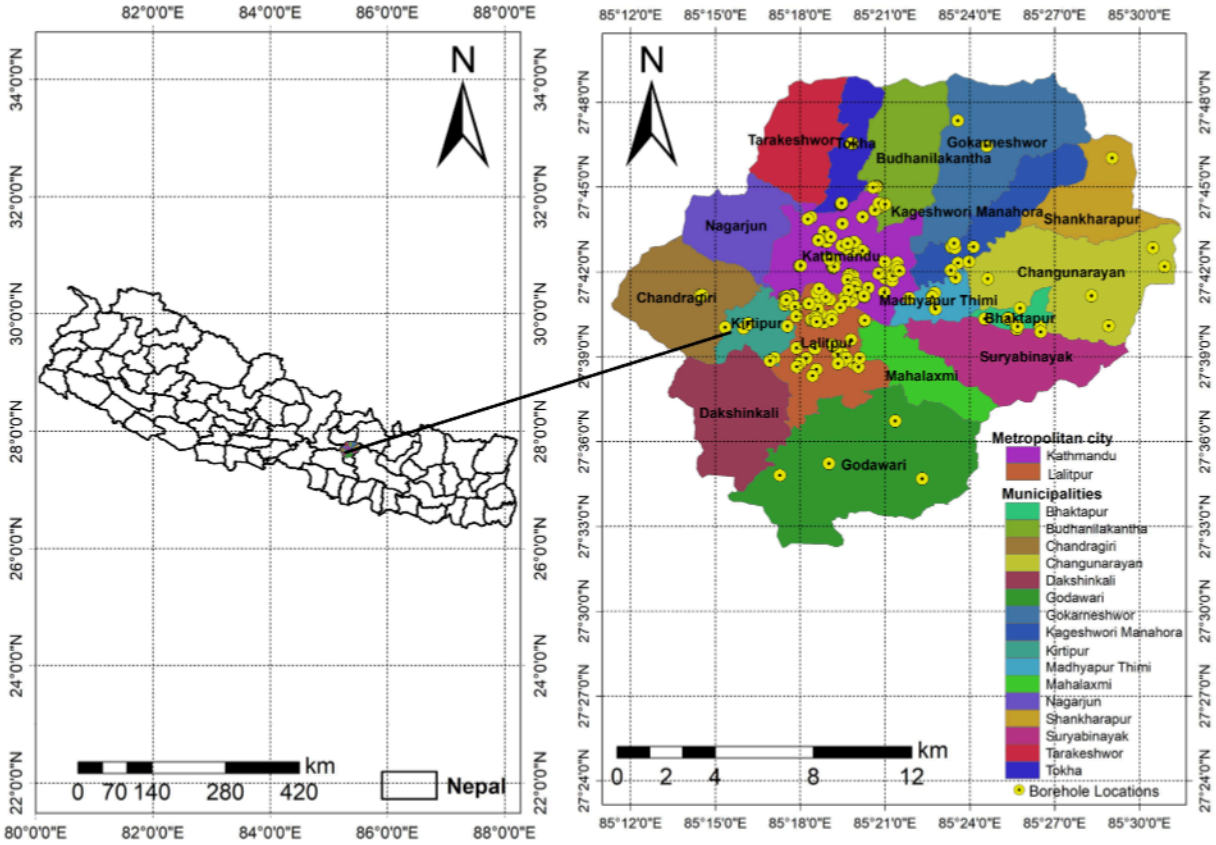

Figure 1. Study area with borehole locations.

Dakshinkali, Suryabinayak, Budhanilkantha, Tokha, Nagarjun, Changunarayan, Bhaktapur, Suryabinayak, Mahalaxmi, and Godawari as depicted in Fig1. In this study, seismic events around 500 km radius of Kathmandu valley have been collected. It extends between 27°31′11″N latitude to 85°00′31″E longitude and covers an area of approximately 633 km^2. The capital of Nepal is home to about 2.9 million people, making it one of the most densely populated areas in the country (National Planning Commission et al., 2022).

The Himalayas are a notable example of a seismotectonic structure, formed by the collision of the Indian and Tibetan tectonic plates. This geological phenomenon is characterized by three primary thrusts are MCT- Main Central Thrust, MBT- Main Boundary Thrust, and MFT- Main Frontal Thrust, which adversely impact the seismic characteristics of the region. These faults extend from north to south, with the MFT system regarded as splinter thrusts originating from the Himalayan thrust. The MFT consists of thrust slices predominantly composed of sedimentary rocks from the Siwalik formation, with several layers of sandstone layers along with conglomerates towards the top. Igneous nappes are commonly observed in the lower Himalayan belt. The MCT, the oldest thrust system, has been active for centuries, while presently, the most active fault is the MBT. Conversely, the MFT is considered as the newest among the three. South of the Main Boundary Thrust (MBT) are the Lesser Himalayas, consisting of sedimentary layers separated by the MBT.

2. Data and Methods

2.1 Seismic Hazard Assessment

In this study, Probabilistic seismic hazard analysis (PSHA) was performed using R-CRISIS software (Ordaz and Salgado-Gálvez, 2020). PSHA is a technique used to assess the possibility and the potential ground motion at a particular location within a defined time frame. PSHA integrates attenuation equations, earthquake recurrence relations, and seismic source zonation to generate seismic hazard curves, which depict the ground motion levels and the corresponding annual frequency of exceeding a certain threshold. For this study,

earthquake catalogues were compiled by amalgamating data from various online platforms, including the US Geological Survey obtained from https://earthquake.usgs.gov, the International Seismological Centre sourced from https://www.seismonepal.gov.np, and the Integrated Research Institutes for Seismology obtained from https://ds.iris.edu/ds/nodes/dmc/data/types/events/catalogs/. The 500 m radius seismo-tectonic zone was taken into consideration when creating the earthquake catalogue, consisting of 4978 seismic events from the years 1960 to 2025. Duplicate events were identified based on matching events, time, depth, location, and magnitude values. Events that appeared in three earthquake catalogs were cross-referenced, and only the most complete entry was retained. Moment magnitude was chosen due to the limitations of other scales such as surface-wave magnitude (M_s), local magnitude (M_l), and body-wave magnitude (M_b), which are applicable wthin specific distance and frequency ranges. M_w provides the most precise assessment for significant earthquakes, but converting other scales to requires empirical correlations particular to each region. Among 4978 seismic events, 320 events were recorded using the Local Magnitude (M_l) scale ranging from 1.7 to 6.5, 2,064 events with the Moment Magnitude (M_w) scale ranging from 1.9 to 7.8, 2591 events with the Body Wave Magnitude (M_b) scale ranging from 1.7 to 6.9, and only 3 events with the Surface Wave Magnitude (M_s) scale (ranging from 5.0 to 6.1). The global relationship used in this study to convert M_s to M_w, M_b to M_w, M_l to M_w were derived using general orthogonal regression analysis in MATLAB. The resulting conversion equations are presented as shown in Eqs. (1), (2) and (3). Similar regression analyses have also been conducted in previous studies by (Das et al., 2012; Ristau, 2009; Wason et al., 2012).

$$M_w = 1.12 + 0.8M_s \qquad (R^2 = 1) \tag{1}$$

$$M_w = 0.695 + 0.851M_b \qquad (R^2 = 0.72) \tag{2}$$

$$M_w = 2.46 - 0.39M_l \qquad (R^2 = 0.51) \tag{3}$$

Dependent seismic events (aftershocks and foreshocks) were removed using Gardner and Knopoff's (1974) declustered algorithm implemented in Zmap software (Wyss et al., 2001). Figure 2 shows the raw and declusterd data (from zmap) considered in this study.

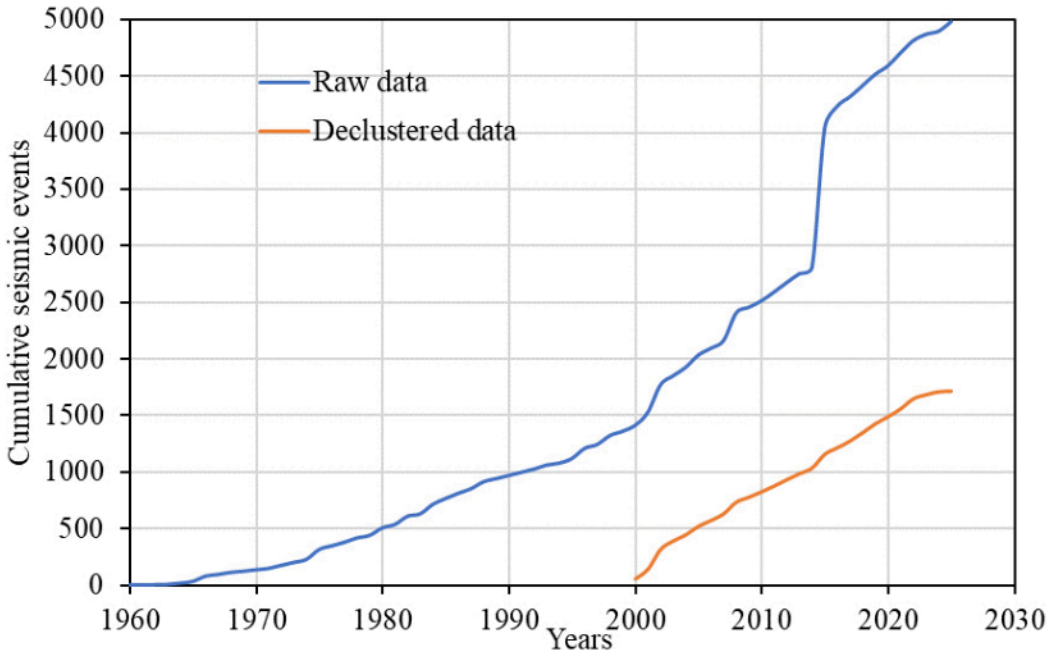

Figure 2. Cumulative number of earthquakes with time.

The seismic catalog was divided into two periods for analysis, pre-2000 and post-2000, to evaluate the changes in completeness. For the pre-2000 period, the standard deviation values exhibited fluctuations but generally showed a decreasing trend over time, indicating completeness in the catalog as it lengthened. For example, the values for M_w 3 to 4 ranged from 1.86 in 1960-1965 to 0.45 in 1960-2010, suggesting a reduction in variability as time progressed. Similarly, for M_w 4 to 5, M_w 5 to 6, and $M_w > 6$, the standard deviations also decreased over time. Specifically, the M_w 4 to 5 values decreased from 1.02 in 1960-1965 to 0.03 in 1960-2010, showing a significant reduction in variability. These trends reflect the catalog improving completeness, with fewer fluctuations as the data set grew and more events were recorded. In contrast, the post-2000 data reveals higher and more fluctuating standard deviation values compared to the pre-2000 period. For M_w 3 to 4, the standard deviations start at 1.93 in 2000-2001 and stabilize at 1.41 by 2000-2025, maintaining higher values compared to the pre-2000 period. For M_w 4 to 5, the values drop from 1.59 in 2000-2001 to 1.29 in 2000-2025, though they show more variability than the earlier period. The M_w 5 to 6 and $M_w > 6$ values are higher in the initial years but stabilize at 1.41 after 2000, especially for $M_w > 6$, which remains constant throughout the post-2000 period. This suggests that while there was more variability in the early years post-2000, the seismic activity began to stabilize as the catalog matured. The observations from the data include the more fluctuating standard deviations in the post-2000 period, particularly in the early years (2000-2009), where the values were larger compared to the pre-2000 period. However, a trend of reducing variability over time can be seen, especially for M_w 3 to 4, M_w 4 to 5, and M_w 5 to 6, indicating that seismic activity may have become more predictable in recent years. For $M_w > 6$, the data shows consistency, with values remaining constant at 1.41 from 2000 to 2025, which suggests limited seismic activity in this category.

The completeness magnitude (M_c) was determined using the Max Curvature method. In Fig. 3, the filled squares represent the number of earthquakes within each magnitude bin, while the empty squares denote the cumulative number of earthquakes with magnitudes equal to or greater than each bin. The solid red lines indicate the best-fit linear regression, and M_c signifies the magnitude of completeness. The completeness of the catalog was assessed employing Stepp's method (Stepp, 1972). The seismic arial source zone was subdivided into fourteen zones, as shown in Fig. 4 depending on their seismicity and statical analysis of earthquake completeness. Each zone was assumed to be seismically uniform, implying that any point within a zone has an equal likelihood of experiencing an earthquake in the future.

In this study, the maximum magnitude (m_{max}) is estimated using Kijko's (1997) method, a probabilistic approach that accounts for the observed earthquake catalog. The earthquake magnitudes are first filtered for each seismic zone to consider only events with M⩾4. Then, within each zone, the earthquake magnitudes are sorted in descending order, and the largest observed magnitude is initially taken as the maximum observed magnitude (M_{obs}). The method is built

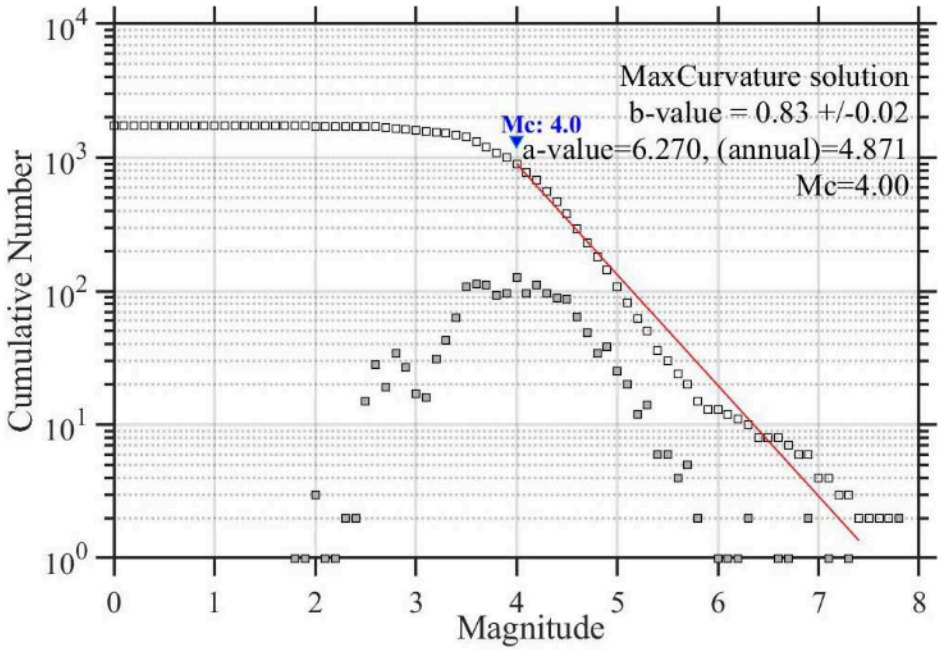

Figure 3. Frequency magnitude distribution using Gardner and Knopoff method.

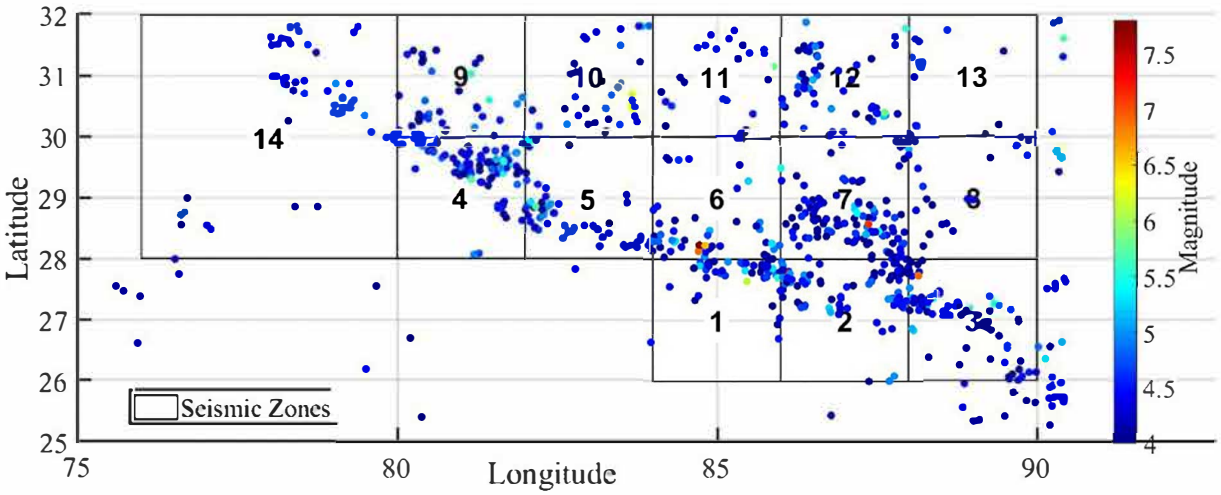

Figure 4. Delineation of seismic source zone.

on the Gutenberg-Richter relationship, which describes the frequency-magnitude distribution of earthquakes. Then, the recurrence parameter b-value, as shown in Eq. (4), is calculated using the maximum likelihood estimation (MLE) method and is tabulated in Table 1. The calculation was performed using earthquakes above the magnitude of completeness (M_c), ensuring a reliable estimation of recurrence parameters.

$$b = \frac{\log_{10}(e)}{M_{\text{mean}} - M_{\text{min}}} \tag{4}$$

where M_{mean} and M_{min} are the mean and minimum observed magnitudes in each zone, respectively. The maximum magnitude (m_{max}) is then determined based on the Kijko probabilistic approach, incorporating the b-value and

Source zones	a	b	m_{max}
1	5.13	0.86	6.1
2	5.67	0.93	7.3
3	5.87	0.99	6.9
4	5.42	0.84	5.7
5	5.90	1.03	5.7
6	4.24	0.63	7.8
7	6.45	1.08	7.1
8	6.32	1.25	5.1
9	5.55	0.99	5.6
10	4.31	0.69	6.7
11	6.23	1.21	5.8
12	5.32	0.89	5.8
13	4.77	0.89	4.9
14	5.20	0.87	5.1

Table 1. Seismic Zone Parameters: Gutenberg Richter coefficients (a, b) and Maximum Magnitude.

earthquake recurrence rates, ensuring that the estimated maximum magnitude accounts for both observed seismicity and potential unobserved extreme events.

Selecting suitable attenuation relationships is crucial for accurate seismic hazard assessment, as noted by (Duglas, 2003). Developing Ground Motion Prediction Equations (GMPEs) becomes challenging in areas where strong motion data are scarce. In such instances, these equations can be borrowed or extrapolated from regions with comparable tectonic characteristics and seismicity. Most parts of the world lack extensive databases of local earthquake recordings, which increases the epistemic uncertainty of any model. In many areas, including those with potential seismic hazards, the absence of region-specific ground-motion models exacerbates this uncertainty. Numerous GMPEs exit for active crustal regions and basins. The details of these GMPEs are provided in Bajaj and Anbazhagan (2018). Bajaj and Anbazhagan (2021) suggested using the GMPE for regions with seismic and tectonic characteristics similar to those of the Himalayas, as it is often used as a proxy in areas with limited local data. Similarly,the study conducted by Rahman et al. (2018), Thapa and Guoxin (2013), and Nath and Thingbaijam (2012) identified that this study region belongs to the active shallow crustal regime (ACR) with many subduction zone interface (SZI) earthquakes across the Himalayas. Moreover, previous hazard studies conducted in Nepal have presumed that the Himalayas and its surrounding regions belong to SZI or ACR. Additionally, the GMPEs developed and relevant to the Himalayan regions included in Bajaj and Anbazhagan (2021) are considered in this study. Based on these findings, this study uses the following attenuation models: Abrahamson and Silva (2014), Campbell and Bozorgnia (2008), Atkinson and Boore (2003), and Youngs et al. (1997). For seismic hazard estimation through PSHA, the entire study region is divided into small grids of size $0.04^{\circ}*0.04^{\circ}$. The study area is initially defined in the software using a shapefile, followed by specifying grid points. Then, seismic sources are demarcated by entering their coordinates and depth. Seismicity parameters such as a, b-values, λ, and m_{max} are the input parameters for each seismic source. The b-value for all the areal source zones is provided for the Valley, and the m_{max} for each source zone is specified. The seismicity parameter M_{min} is considered as M_w 4. Subsequently, the attenuation relationships for each source zone are chosen. The four GMPEs for PGA are entered into the R-CRISIS program. Due to the absence of significant observed data to evaluate the weighting of each source model, equal weights of 0.25 were assigned to them. The outcomes are generated in the form of PGA for selected return periods. Additionally, hazard curves are generated at each grid point. The vulnerability index map based on the dominant frequency and soil amplification factor was described in Poudyal et al., (2024) where the urban part of the Kathmandu Valley is considered in this study. Thus a comprehensive seismic risk assessment was conducted through the integration of a newly conducted probabilistic seismic hazard analysis (PSHA) and a soil vulnerability index map by Poudyal et al. (2024) at municipal and metropolitan cities, and the risk zones were classified as Low, Medium and High zones using the Jenks Natural Break classification method by classifying and ranking between 1 and 5 provided in ArcGIS at 10% probability of exceedance in 50years for the return period of 475 year.

3. Result and Analysis

In this study, the PSHA results presented as a PGA map on bedrock with a 10% probability of exceedance, to a 475-year return period (Fig. 5) and the vulnerability index for municipalities and metropolitan cities, depicted in Fig. 6 as are both tabulated in Table 2, with vulnerability index sourced from (Poudyal et al., 2024).

The analysis of the PGA values and the vulnerability index (K_g) across various municipalities and metropolitan cities reveal distinct differences in seismic risk profiles. In Kathmandu Metropolitan City, the Peak Ground Acceleration value ranges from 0.345 to 0.356 g, indicating moderate seismic activity. However, the vulnerability index varies widely from 0.21 to 15.07, suggesting that while the ground shaking may be moderate, certain areas within Kathmandu are highly vulnerable to seismic damage due to factors like poor construction quality and very soft soil conditions. Similarly, Lalitpur metropolitan city shows a comparable PGA range (0.345 to 0.354 g) but has a higher maximum vulnerability index (0.40 to 21.72), implying that Lalitpur may have regions that are even more susceptible to seismic risks compared to Kathmandu. In Bhaktapur Municipality and Madhyapur Thimi Municipality, the PGA values are slightly higher (0.363 to 0.375 g and 0.353 to 0.364 g, respectively), but their vulnerability indexes are lower (0.87 to 3.29 and 0.50 to 2.96). This suggests that these municipalities, while exposed to moderate seismic shaking, have relatively lower vulnerability, possibly due to better building practices or more stable ground conditions. Kirtipur Municipality and Godawari Municipality display similar PGA ranges (0.348 to 0.365 g), but the vulnerability index of Godawari (1.31 to 6.48) is broader, indicating a greater disparity in seismic resilience across the area.

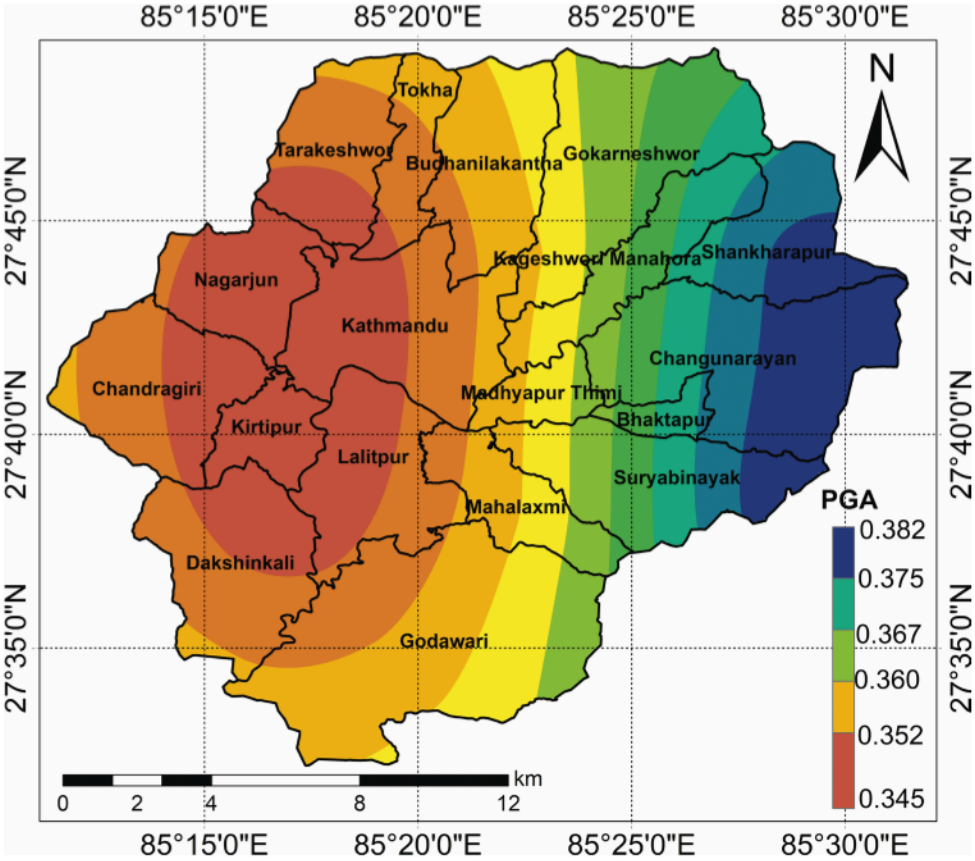

Figure 5. Bedrock PGA at 10% probability of exceedance.

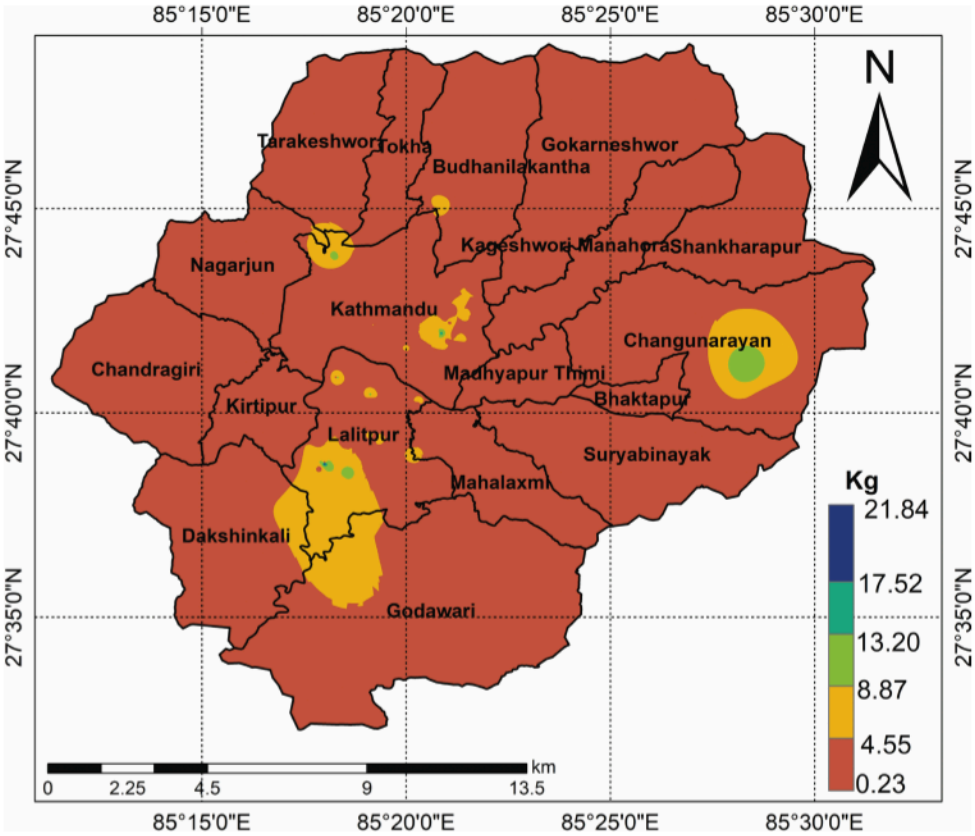

Figure 6. Vulnerability index map.

Locations	PGA (g)	K_g
Kathmandu Metropolitan City	0.345-0.356	0.21-15.07
Lalitpur Metropolitan City	0.345-0.354	0.40-21.72
Bhaktapur Municipality	0.363-0.375	0.87-3.29
Madhyapur Thimi Municipality	0.353-0.364	0.50-2.96
Kirtipur Municipality	0.348-0.356	0.61-3.88
Godawari Municipality	0.349-0.365	1.31-6.48
Mahalaxmi Municipality	0.350-0.367	1.66-6.09
Changunarayan Municipality	0.362-0.382	0.93-12.12
Suryabinayak Municipality	0.355-0.382	1.30-2.69
Shankharapur Municipality	0.369-0.380	1.50-4.28
Gokarneshwor Municipality	0.354-0.373	0.87-3.89
Budhanilkantha Municipality	0.350-0.360	1.02-15.17
Tokha Municipality	0.347-0.356	0.79-6.11
Nagarjun Municipality	0.345-0.350	0.75-7.06
Chandragiri Municipality	0.345-0.354	0.73-3.45
Dakshinkali Municipality	0.346-0.354	0.90-6.23
Tarakeshwor Municipality	0.346-0.355	1.41-5.27
Kageshwori Manohara Municipality	0.355-0.375	0.6-4.01

Table 2. PGA and K_g of Kathmandu Valley.

Mahalaxmi Municipality and Changunarayan Municipality exhibit moderate to high PGA values (0.350 to 0.382 g). The vulnerability index of Mahalaxmi municipality ranges from 1.66 to 6.09, whereas Changunarayan municipality ranges from 0.93 to 12.12, highlighting that Changunarayan may have areas of higher vulnerability despite experiencing similar levels of ground shaking. Suryabinayak Municipality and Shankharapur Municipality also present relatively high PGA values (0.355 to 0.382 g and 0.369 to 0.380 g, respectively). However, the lower vulnerability index range of Suryabinayak municipality (1.30 to 2.69) suggests better resilience to seismic damage, while the wider range of Shankharapur municipality (1.50 to 4.28) indicates a higher risk of structural damage in the event of an earthquake. Municipalities like Gokarneshwor and Budhanilkantha show moderate PGA values (0.354 to 0.373 g and 0.350 to 0.360 g, respectively), but Budhanilkantha has a significantly higher vulnerability index range (1.02 to 15.17). This indicates that some areas in Budhanilkantha might be at substantial risk, even if the

ground shaking intensity is not the highest. On the other hand, Tokha, Nagarjun, Chandragiri, and Dakshinkali Municipalities have relatively low to moderate PGA ranges (0.345 to 0.356 g) with varying vulnerability indexes. For example, Tokha and Nagarjun have moderate vulnerability with maximum K_g values of 6.11 and 7.06, while Chandragiri has a lower vulnerability index (0.73 to 3.45), suggesting less potential for seismic damage. Lastly, Tarakeshwor Municipality and Kageshwori Manohara Municipality exhibit moderate PGA ranges (0.346 to 0.375 g) with vulnerability indexes of 1.41 to 5.27 and 0.6 to 4.01, respectively. This comparison indicates that while the seismic shaking intensity might be similar, Tarakeshwor has a slightly higher potential for damage due to a greater vulnerability index. Figure 7 illustratesthe classification of seismic risk zones across various municipalities and metropolitan cities as determined by integrating the Peak Ground Acceleration (PGA) and vulnerability index map.

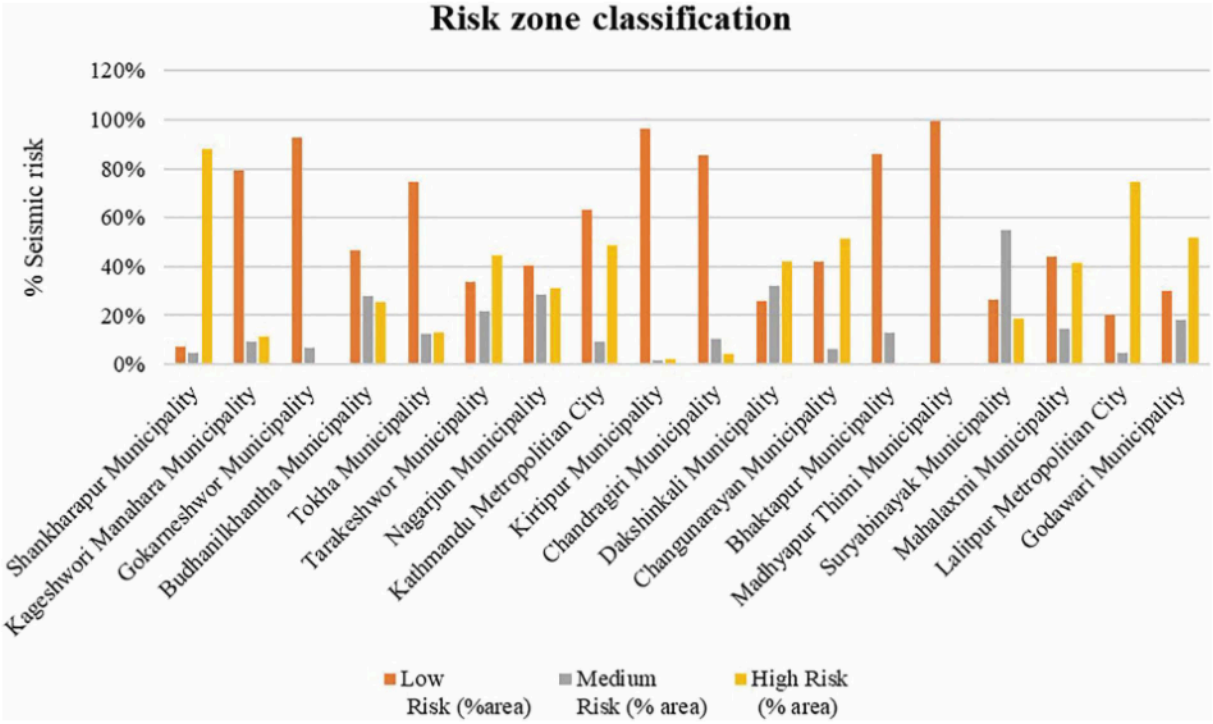

Figure 7. Risk zone classification.

The data reflects the proportion of each municipality area that falls into low, medium, and high-risk seismic zones. The risk zones are classified into three zones as shown in Fig. 8.

In Budanilkantha Municipality, particularly in the Basbari area, the soil composition, i.e., sandy silt and subsequent layers of sand and silt, contributesto a differentiated risk profile. A significant portion of the municipality is classified as low risk, but there are notable areas categorized as medium and high risk, with 46.65% of its area classified as low risk, 28.07% as medium risk, and 25.27% as high risk across the region. Tokha Municipality, particularly in the Dhapasi area, exhibits soil characteristics of medium to dense, poorly graded sand. These soil properties correlate with a significant proportion of the area being classified as low risk, with only small areas designated as medium and high risk. The majority of its area experiences the low-risk category, comprising 74.50%, with smaller proportions in mmedium-risk (12.43%) and high-risk (13.07%) zones. The nature of poorly graded sand, which offers greater stiffness and shear strength, is likely a contributing factor to the lower risk levels observed in this municipality. Kageshwori Municipality, particularly in the Mulpani area, is characterized by silty sand, which contributes to the low amplification of seismic waves and relatively low structural vulnerabilities. Additionally, 9.65% of the area falls within the medium-risk category, indicating moderate susceptibility to seismic hazards. However, a noteworthy 11.26% of the territory of municipality is classified as high risk, emphasizing the community resilience against potential seismic events This area predominantly falls within the low-risk category, with only a small percentage designated as medium and high risk, indicating a significant portion of the municipality is relatively safer from seismic hazards.

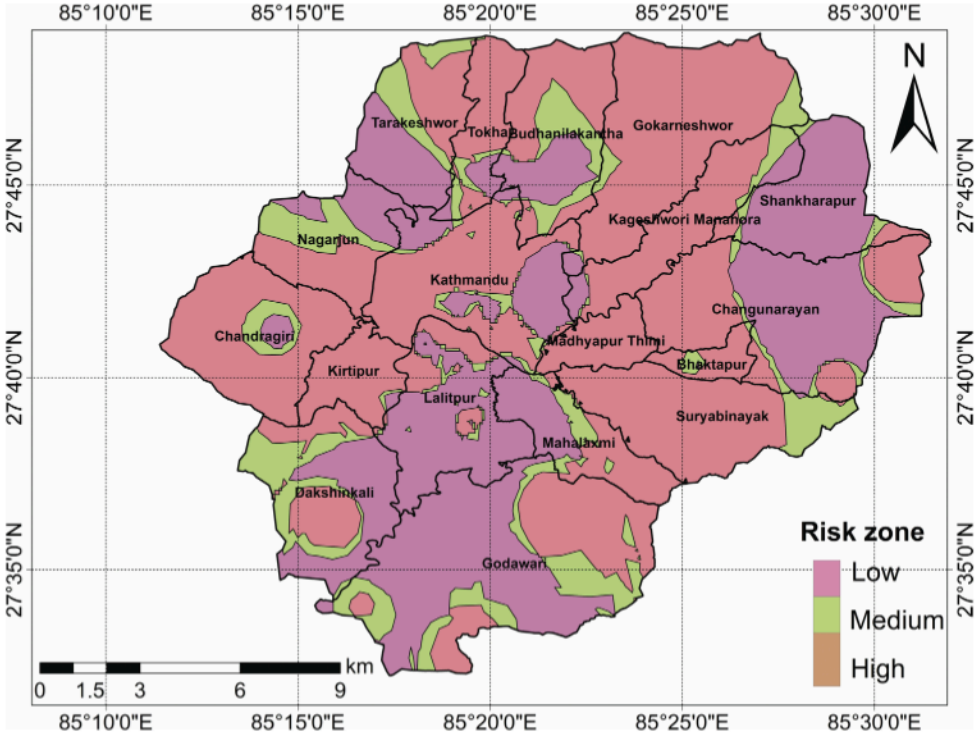

Figure 8. Seismic risk zone.

Both Changunarayan and Bhaktapur municipalities are located in the eastern part of the Kathmandu Valley. In Bhaktapur Municipality, the study reveals a relatively lower proportion of the area classified as high risk compared to neighboring municipalities standing at only 0.84%. In Changunarayan municipality, 51.54%of the area is classified as high risk, indicating a substantial vulnerability to seismic hazards. Despite its location in the same geographical region, Bhaktapur exhibits a significantly lower susceptibility to seismic hazards, while Changunarayan Municipality shows a much higher proportion of its area classified as high risk. This contrast underscores the importance of localized geological factors in determining seismic risk. Madhyapur Thimi Municipality stands out with nearly all of its area classified as low risk (99.38%), making it one of the safer regions in terms of seismic hazards within the Kathmandu Valley. The study supports previous findings that areas with soft soils, such as Bhaktapur and Thimi, are more prone to local amplification, which can lead to significant damage during earthquakes. Gokarneshwor Municipality, specifically in the Sundarijal area, 92.49% is classified as low risk, while only 6.85% falls into the medium-risk category, and a mere 0.66% is designated as high risk. In Kirtipur Municipality, the presence of bedrock exposure correlates with a low susceptibility to seismic hazards with a staggering 96.34% of its area falling into the low-risk category. The Gurjudhara area, located southwest part of the valley, within Chandragiri Municipality, is characterized by blackish medium dense silty Clay. Despite Chandragiri municipality predominantly falling into the low-risk category, with 85.1% of its area classified as such, it contains pockets of higher vulnerability, such as the Gurjudhara area, necessitating targeted risk mitigation efforts. The soil properties in Suntol, located northeast of Kathmandu Valley in Shankharapur Municipality, raise significant concerns about earthquake vulnerability. This area is characterized by silt and clay, which tend to amplify seismic waves. While a small portion (11.98%) falls under low and medium risk categories, a staggering 88.01% of the municipality, which includes Suntol and its population of 29,318 (National Planning Commission et al., 2022) is designated as high risk which includes Suntol and its population, is designated as high risk.

Both Godawari and Dakshinkali, located in the southern part of the Kathmandu Valley, exhibit varying degrees of seismic risk. In Godawari, approximately 29.88% of the area is classified as low risk, indicating a considerable portion of relatively safer zones. However, a noteworthy 51.88% of the territory falls within the high-risk category, highlighting significant susceptibility to seismic hazards in this region. Dakshinkali municipality particularly the Hattiban area consists of sandy gravel soil followed by medium clayey silt of Low plasticity. While the presence of sandy gravel offers some advantages, the amplifying effect of the lower layer and the overall vulnerability variation necessitate a more detailed assessment. Hattiban area presents a different risk profile, with 25.84% of

the area classified as low risk, suggesting relatively fewer safer zones compared to Godawari. However, Dakshinkali shows a higher proportion of medium-risk areas, accounting for 32.28% of the municipality's territory. Additionally, 41.87% of Dakshinkali is classified as high risk, indicating a significant susceptibility to seismic hazards similar to Godawari. Overall, while both locations share a southern geographic position within the Kathmandu Valley, they exhibit differences in the distribution of seismic risk levels, with Godawari showcasing a higher proportion of high-risk areas compared to Dakshinkali. Mahalaxmi municipality, located in the southeast part of the Kathmandu Valley, demonstrates a seismic risk distribution with 44.16% of its area falling into the medium-risk category, 14.39% in the high-risk category, and 41.45% in the low-risk category. In contrast, Suryabinayak municipality, also situated in the southeast region, exhibits a different risk profile with a higher proportion of its area classified as medium risk (55.04%), followed by 26.29% in the low-risk category and 18.67% in the high-risk category. Similarly, Nagarjuna municipality, located in the northwest part of the Kathmandu Valley, demonstrates a seismic risk distribution with 40.36% of its area falling into the medium-risk category, 28.36% in the high-risk category, and 31.28% in the low-risk category. This seismic risk profile of this municipality suggests a relatively balanced distribution across the three risk categories, indicating the need for comprehensive risk mitigation strategies to address the varying levels of vulnerability within the region.

Approximately 74.68% of the Lalitpur area falls into the high-risk category, indicating a significant vulnerability to seismic hazards. Overall, Lalitpur Metropolitan City emerges as the municipality with the highest seismic risk among the four central Kathmandu areas, followed by Madhapur Thimi, Kathmandu Metropolitan City, and Kirtipur Municipality respectively. The seismic risk assessment across the central Kathmandu areas reveals notable disparities in vulnerability levels, with Lalitpur Metropolitan City emerging as the municipality with the highest seismic risk. Kathmandu Metropolitan City, while still exhibiting considerable risk, has a proportion of its area classified as high risk, at 48.66%

4. Discussion

The seismic risk assessment conducted across various municipalities within the Kathmandu Valley reveals significant variations in vulnerability. The analysis shows that Lalitpur Metropolitan City emerges as the municipality with the highest seismic risk, with approximately 74.68% of its area classified as high risk. Conversely, Madhyapur Thimi Municipality stands out with nearly all of its area (99.38%) classified as low risk, making it one of the safer regions within the valley which is justified by the study carried out by Bijukchhen et al. (2017). Other municipalities, such as Changunarayan and Godawari, also exhibit a substantial proportion of their area classified as high risk, underscoring the uneven distribution of seismic vulnerability across the region.

The variations in seismic risk across different municipalities highlight the critical role of localized geological factors. For instance, Bhaktapur and Madhyapur Thimi, despite being located nearby, show stark differences in risk levels, with Bhaktapur having a significantly higher proportion of high-risk areas compared to Madhyapur Thimi. This discrepancy can be attributed to the underlying soil composition and the amplification of seismic waves, which differ between the two municipalities. In contrast, municipalities like Kirtipur and Gokarneshwor exhibit a predominantly low-risk profile as presented by Poudyal et al. (2024), which can be linked to the presence of bedrock exposure and stiffer soil materials, offering greater resistance to seismic forces.

Hashash et al. (2015) observed the liquefaction site near Mulpani, located approximately 1.5 km southeast of Changunarayan on the same floodplain. This site vividly demonstrated the impact of seismic activity on agricultural land, particularly in areas prone to liquefaction. Sharma et al. (2019) highlighted that the Mulpani area, which lies close to significant geological features, showed how earthquake-induced liquefaction can disrupt farming activities and damage agricultural yields, as observed with the carrots and potatoes that were ejected from the ground during the earthquake. Additionally, JICA (2018) documented the landslides on the northern slope of Changunarayan, north of Suryabinayak, highlighting the susceptibility of the region to slope instability in the aftermath of seismic events. Also Hashash et al. (2015) presented the Hattiban site as a unique case of liquefaction, distinct from other locations assessed by the GEER team. Unlike typical liquefaction sites that often serve as borrow pits for sand extraction, Hattiban exhibited numerous sand boils, indicating significant subsurface disturbance during seismic events. The auger investigation conducted at this site revealed a detailed subsurface stratigraphy that likely contributed to the observed liquefaction phenomena. This included a low plasticity silt or silty clay layer, a black cotton clay layer, and a fine sand layer beneath, with the groundwater table found at 2.5 meters below the ground

surface. The findings from Hattiban underscore the complexity of subsurface conditions that can exacerbate liquefaction risks.

Pokhrel et al. (2022) identified the lateral spreading and surface cracks in Nagarjuna municipality and further highlighted the seismic risks associated with the topography of the area and geological conditions. The surface crack, which measured approximately 170 feet in length, is likely due to slope stability issues rather than a more extensive or deep-seated fault rupture. The steep slopes and variable soil compositions make it particularly vulnerable to slope failures, especially during or after seismic events. This localized ground movement suggests the need for targeted slope stabilization measures to prevent future occurrences and reduce the risk of landslides in the area. Severe damage was reported by Ghimire et al. (2020) in regions where Kalimati Clay is prevalent, specifically in Patan Durbar Square, Kathmandu Durbar Square, and Bhaktapur Durbar Square. These areas, identified as the Peak Destruction Zone, underscore the significant role that local soil conditions play in amplifying seismic impacts. Likewise.

The findings of this study have profound implications for urban planning and disaster preparedness in the Kathmandu Valley. High-risk municipalities such as Lalitpur, Changunarayan, and Godawari should be prioritized for immediate intervention measures. This could include the implementation of stricter building codes, the retrofitting of existing structures, and the development of emergency response plans tailored to the specific risk profiles of these areas. Furthermore, areas with a significant portion of low-risk zones, like Madhyapur Thimi and Kirtipur, should not become complacent but should instead use their current status to reinforce resilience and preparedness for future seismic events.

While the study provides a comprehensive overview of seismic risk distribution, certain limitations must be acknowledged. It does not account for socio-economic factors that could also influence the overall vulnerability of the population. Future research could benefit from integrating these aspects to provide a more holistic assessment of seismic risk. Additionally, more detailed site-specific studies could offer insights into micro-level variations within municipalities, leading to more targeted risk mitigation strategies. In the broader context of seismic risk management in Nepal, this study underscores the need for localized approaches to disaster preparedness. The Kathmandu Valley, being one of the most densely populated and urbanized regions in Nepal, faces unique challenges that require urgent attention. The results of this study are particularly relevant for policymakers and urban planners tasked with safeguarding the region's population against the inevitable threat of future earthquakes. By incorporating these findings into the planning process, the resilience of the Kathmandu Valley can be significantly enhanced, potentially saving countless lives and reducing the economic impact of future seismic events.

5. Conclusions

In this study, the integration of probabilistic seismic hazard and vulnerability index map provides a comprehensive picture of earthquake risk in the area. The significance of earthquake threats throughout the Kathmandu Valley is highlighted by the findings, which are depicted in the form of risk zone. This integrated approach explores the complex interplay of geological elements and acknowledges that seismic risk extends beyond PGA values. Notably, Madhyapur Thimi emerged as the most secure region, with an overwhelming 99.38% of its area classified as low-risk, whereas Shankharapur Municipality was identified as highly vulnerable, with 88.01% of its region falling into the high-risk category. Conversely, areas like Kirtipur Municipality demonstrate lower vulnerability, attributed to bedrock exposure and less amplification. These findings emphasize the critical need for targeted risk mitigation strategies for the specific vulnerabilities of each municipality. By combining seismic hazard data with the vulnerability index, this study provides a more nuanced and actionable framework for earthquake risk management in the Kathmandu Valley. It is essential to incorporate dynamic factors such as land use changes and ongoing urban development into future assessments. Continuous updating and refinement of seismic risk evaluations will enhance the resilience of communities and support informed decision-making for disaster preparedness and urban planning in this seismically active region.

Data availability statement. The datasets supporting the findings of this study are available from the first author upon request and with permission from various soil testing laboratories, including EverSafe Engineering Consultancy, Prime Civil Lab, and Multi Lab Pvt.

Acknowledgements. The datasets supporting the findings of this study are available from the first author upon request and with permission from various soil testing laboratories, including Eversafe Engineering Consultancy, Prime Civil Lab, and Multi Lab Pvt.

References

Anbazhagan, P., K. Bajaj and S. Patel (2015). Seismic hazard maps and spectrum for Patna considering region-specific seismotectonic parameters, Nat. Hazards, 78, 3, 1753-1774, doi:10.1007/s11069-015-1764-0.

Anbazhagan, P., K. Bajaj, N. Dutta, S. S. R. Moustafa et al. (2017). Region-specific deterministic and probabilistic seismic hazard analysis of Kanpur city, J. Earth Syst. Sci., 126, 1, doi:10.1007/s12040-016-0779-6.

Anbazhagan, P., K. Bajaj, K. Matharu, S. S. R. Moustafa et al. (2019). Probabilistic seismic hazard analysis using the logic tree approach-Patna district (India), Nat. Hazards Earth Syst. Sci., 19, 10, 2097-2115, doi:10.5194/nhess-19-2097-2019.

Bajaj, K. and P. Anbazhagan (2018). Determination of GMPE functional form for an active region with limited strong motion data: application to the Himalayan region, J. Seismol., 22, 1, 161-185, doi:10.1007/s10950-017-9698-5.

Bajaj, K. and P. Anbazhagan (2021). Detailed Seismic Hazard, Disaggregation and Sensitivity Analysis for the Indo-Gangetic Basin, Pure Appl. Geophys., 178, 6, 1977-1999, doi:10.1007/s00024-021-02762-7.

Bhochhibhoya, S. and R. Maharjan (2022). Integrated Seismic Risk Assessment in Nepal, Nat. Hazards Earth Syst. Sci., 22, 10, 3211-3230, doi:10.5194/nhess-22-3211-2022.

Bhusal, B. and H. R. Parajuli (2019). Probabilistic Seismic Hazard Analysis for Nepal Using Areal and Longitudinal Faults Source, Proceddings of IOE Graduate Conference, 6, 125-132, 2350-8914 (Online), 2350-8906 (Print).

Bhusal, B., M. Aaqib, S. Paudel and H. R. Parajuli (2022). Site specific seismic hazard analysis of monumental site Dharahara, Kathmandu, Nepal. Geomatics, Nat. Hazards Risk, 13, 1, 2674-2696, doi:10.1080/19475705.2022.2130109.

Bijukchhen, S., N. Takai, M. Shigefuji, M. Ichiyanagi and T. Sasatani (2017). Strong-motion characteristics and visual damage assessment around Seismic stations in Kathmandu after the 2015 Gorkha, Nepal, earthquake, Earthquake Spectra, 33, 1, S219-S242, doi:10.1193/042916EQS074M.

Das, R., H. R. Wason and M. L. Sharma (2012) Temporal and spatial variations in the magnitude of completeness for homogenized moment magnitude catalogue for northeast India, J. Earth Syst. Sci, 121, 1, 19-28, doi:10.1007/s12040-012-0144-3.

Douglas, J. (2003). Earthquake ground motion estimation using strong-motion records: A review of equations for the estimation of peak ground acceleration and response spectral ordinates, Earth-Sci. Rev., 61, 1-2, 43-104, doi:10.1016/S0012-8252(02)00112-5.

Hashash, Y. M. A., B. Tiwari, R. E. S. Moss, D. Asimaki et al. (2015). Geotechnical Field Reconnaissance : Gorkha (Nepal) Earthquake of April 25 2015 and Related Shaking Sequence, Geotechnical Extreme Event Reconnaissance, Geotechnical Extreme Event Reconnaissance Association (GEER), Berkeley, CA.

JICA (2018). Federal Democratic Republic of Nepal the Project for Assessment of Earthquake Disaster Risk for the Kathmandu Valley, Final Report, 2 : Main Report, in Final Report, Japan International Cooperation Agency (JICA), Kathmandu.

Khatakho, R., D. Gautam, K. R. Aryal, V. P. Pandey et al. (2021). Multi-hazard risk assessment of kathmandu valley, Nepal, Sustainability (Switz.), 13,10, doi:10.3390/su13105369.

Nath, S. K. and K. K. S. Thingbaijam (2012). Probabilistic seismic hazard assessment of India, Seismol. Res. Lett., 83, 1, 135-149, doi:10.1785/gssrl.83.1.135.

National Planning Commission, Statistics, C. B. of, and Nepal (2022). Nepal Census 2021. Retrieved from https://censusnepal.cbs.gov.np/Home/Details?tpid=9.

NBC 105 (2020). Seismic Design of Buildings in Nepal. Retrieved from https://www.dudbc.gov.np/uploads/default/files/9a192ea8b7e1c45b99628f0869052201.pdf.

Ordaz, M. and M. A. Salgado-Gálvez (2020). R-CRISIS Validation and Verification Document Program for Probabilistic Seismic Hazard Analysis, Universidad Nacional Autónoma de México, Universidad Nacional Autónoma de México, Mexico City.

Parajuli, H. R., B. Bhusal and S. Paudel (2021). Seismic zonation of Nepal using probabilistic seismic hazard analysis, Arab. J. Geosci., 14, 20, doi:10.1007/s12517-021-08475-4.

Pokhrel, R. M., C. E. L. Gilder, P. J. Vardanega, F. De Luca et al. (2022). Liquefaction potential for the Kathmandu Valley, Nepal: a sensitive study, Bull. Earthq. Eng. 20, 1, 25-51. doi:10.1007/s10518-021-01198-7.

Poudyal, D., N. Norhaina, R. S. N. Aliaa, B. Kumar Dahal et al. (2024) Spatial mapping of the seismic vulnerability index in Kathmandu Valley: insight from dominant frequency and amplification factor, J. Geophys. Eng., 21, 4, 1272-1285, doi:10.1093/jge/gxae069.

Pradhan, P. M., S. P. Timalsina and M. R. Bhatt (2020). Probabilistic seismic hazard analysis for Nepal, Lowland Technol. Int., 22, 1, 75-80, doi:10.3126/jiee.v2i1.36676.

Rahman, M. Moklesur, L. Bai, N. G. Khan and G. Li (2018). Probabilistic Seismic Hazard Assessment for Himalayan-Tibetan Region from Historical and Instrumental Earthquake Catalogs, Pure Appl. Geophys., 175, 2, 685-705, doi:10.1007/s00024-017-1659-y.

Rahman, Moklesur Md and L. Bai (2018). Probabilistic seismic hazard assessment of Nepal using multiple seismic source models, Earth Planet. Phys., 2, 4, 327-341, 10.26464/epp2018030.

Ristau, J. (2009). Comparison of magnitude estimates for New Zealand earthquakes: Moment magnitude, local magnitude, and teleseismic body-wave magnitude, Bull. Seismol. Soc. Am. 99, 3, 1841-1852, doi:10.1785/0120080237.

Sharma, K., L. Deng and D. Khadka (2019). Reconnaissance of liquefaction case studies in 2015 Gorkha (Nepal) earthquake and assessment of liquefaction susceptibility, Int. J. Geotech Eng., 13, 4, 326-338, doi:10.1080/19386362.2017.1350338.

Stepp, J. C. (1972). Analysis of completeness of the earthquake sample in the Puget Sound area and its effect on statistical estimates of earthquake hazard, Proc. 1st Int. Conf. Microzon., 2, 1, 897-910, https://www.resolutionmineeis.us/documents/stepp-1972.

Stevens, V. L., S. N. Shrestha and D. K. Maharjan (2018). Probabilistic seismic hazard assessment of Nepal, Bull. Seismol. Soc. Am., 108, 6, 3488-3510, doi:10.1785/0120180022.

Thapa, D. R. and G. W. Guoxin (2013). Probabilistic seismic hazard analysis in Nepal, Earthq. Eng. Eng. Vibration, 12, 4, 577-586, doi:10.1007/s11803-013-0191-z.

Thapa, N., K. Pandey, S. Ghimire and K. Acharya (2020). Frequency Dependent Damage Pattern in Kathmandu Valley Due to Mw 7.8 Gorkha Earthquake, J. Geol. Geophys., 9, 4, 1-6, doi:10.35248/2381-8719.20.9.471.

Wason, H. R., R. Das and M. L. Sharma (2012). Magnitude conversion problem using general orthogonal regression, Geophys. J. Int., 190, 2, 1091-1096, doi:10.1111/j.1365-246X.2012.05520.x.

Woessner, J. and S. Wiemer (2005). Assessing the quality of earthquake catalogues: Estimating the magnitude of completeness and its uncertainty, Bull. Seismol. Soc. Am., 95, 2, 684-698, doi:10.1785/0120040007.

Wyss, M., S. Wiemer and R. Zúñiga (2001). ZMAP: A tool for analyses of seismicity patterns, typical applications and uses, Writing, 64.

***CORRESPONDING AUTHOR: Dibyashree POUDYAL**,
Infrastructure University Kuala Lumpur, Department of Civil Engineering, Kajang, Malaysia
e-mail: 082101900007@s.iukl.edu.my